

# From Manipulation of Giant Magnetoimpedance in Thin Wires to Industrial Applications

A. Zhukov · M. Ipatov · C. Garcia · M. Churyukanova ·  
S. Kaloshkin · V. Zhukova

Received: 31 October 2012 / Accepted: 1 December 2012 / Published online: 22 December 2012  
© Springer Science+Business Media New York 2012

**Abstract** We present results on our studies of soft magnetic properties and Giant magnetoimpedance, GMI, effect in thin microwires at elevated frequencies paying special attention to tailoring the GMI effect and achievement of high GMI effect with low hysteretic behavior. We measured magnetic field,  $H$ , dependence of real part, of the longitudinal wire impedance up to frequency,  $f$ , 4 GHz in Co-rich microwires. Amorphous microwires of appropriate composition exhibit extremely soft magnetic properties with low coercivity (generally below 10 A/m) with well defined magnetic anisotropy field,  $H_k$ . We report a number of interesting for sensor applications phenomena such as stress-impedance effect and stress sensibility of overall hysteresis loop shape. Field dependence of the off-diagonal voltage response of pulsed GMI effect in nearly-zero magnetostriction ( $\lambda_s \approx -3 \times 10^{-7}$ ) microwires exhibits anti-symmetrical shape, suitable for industrial applications. We observed that the magnetic field dependence of GMI ratio can be tailored either controlling magnetoelastic anisotropy

of as-prepared microwires or by heat treatment. Composite character of such microwires results in the appearance of additional magnetoelastic anisotropy. We found that if the surface anisotropy is not circumferential, then the magnetization, and consequently, the MI curve  $Z(H)$  present hysteresis. This hysteresis can be suppressed by application of sufficiently high DC bias current  $I_B$  that creates a circumferential bias field  $H_B$ .

**Keywords** Magnetic microwires · Giant magnetoimpedance · Magnetoelastic anisotropy

## 1 Introduction

Soft magnetic materials continue playing an important role in modern industries owing to many important technological applications. Among different families of soft magnetic materials, magnetically soft thin wires (with typical diameters from 1 to 120  $\mu\text{m}$ ) attract considerable interest owing to unusual magnetic properties exhibiting by amorphous ferromagnetic wires such as magnetic bistability and giant magnetoimpedance, GMI, effect [1–3]. These properties are quite attractive for the magnetic sensor applications.

One of the recent tendencies related with development of industrial applications is the miniaturization of the magnetic sensors. Consequently, soft magnetic wires with reduced dimensionality and outstanding magnetic characteristics, such as melt extracted wires (typically with diameters of 40–50  $\mu\text{m}$ ) [4, 5] and glass-coated microwires with even thinner diameters (between 1–40  $\mu\text{m}$ ) [6, 7] recently gained much attention. The advantage of the Taylor–Ulitsky method allowing the fabrication of glass-coated metallic microwires consists of controllable fabrication of long (up to few km long continuous microwire) and homogeneous thin composite wires.

---

A. Zhukov (✉) · M. Ipatov · V. Zhukova  
Dpto Física de Materiales, Facultad de Químicas, UPV/EHU,  
10018, San Sebastián, Spain  
e-mail: [arkadi.joukov@ehu.es](mailto:arkadi.joukov@ehu.es)

V. Zhukova  
e-mail: [valentina.zhukova@ehu.es](mailto:valentina.zhukova@ehu.es)

A. Zhukov  
IKERBASQUE, Basque Foundation for Science, 48011 Bilbao,  
Spain

C. Garcia  
Bogazici Univ, Dept Phys, 34342 Istanbul, Turkey

M. Churyukanova · S. Kaloshkin  
National University of Science and Technology “MISIS”,  
Moscow 119049, Russia

Recently, certain progress on improvement of soft magnetic properties and achievement of high GMI effect of glass coated microwires has been reported at the laboratory level [7]. This gives rise to development of industrial applications for low magnetic field detection in various industrial sectors [6, 8].

GMI effect consists of large sensitivity of the impedance of magnetically soft conductor on applied magnetic field. GMI effect has been successfully explained in the terms of classical electrodynamics through the influence of magnetic field on penetration depth of electrical current flowing through the magnetically soft conductor [9, 10]. Excellent magnetic field sensitivity of GMI effect is suitable for low magnetic field detection. Cylindrical shape and high circumferential permeability observed in amorphous wires are quite favorable for the achievement of a high GMI effect [4, 7–10]. As a rule, better soft magnetic properties are observed for nearly-zero magnetostrictive compositions. It is worth mentioning that the magnetostriction constant,  $\lambda_s$ , in system  $(\text{Co}_x\text{Fe}_{1-x})_{75}\text{Si}_{15}\text{B}_{10}$  changes with  $x$  from  $-5 \times 10^{-6}$  at  $x = 1$ , to  $\lambda_s \approx 35 \times 10^{-6}$  at  $x \approx 0.2$ , achieving nearly-zero values at Co/Fe about 70/5 [11].

It was pointed out [2–6] that the good magnetic softness is directly related to the GMI effect: The magnetic field dependence of the GMI spectra is mainly determined by the type of magnetic anisotropy. Thus, the circumferential anisotropy leads to the observation of the maximum of the real component of wire impedance (and consequently of the GMI ratio) as a function of the external magnetic field. On the other hand, in the case of axial magnetic anisotropy, the maximum value of the GMI ratio corresponds to zero magnetic fields [2–6], i.e., results in a monotonic decay of the GMI ratio with the axial magnetic field. Afterward, the “scalar” model of GMI effect was significantly modified taking into account the tensor origin of the magnetic permeability and magnetoimpedance [12–15]. Consequently, nondiagonal components of the magnetic permeability tensor and impedance tensor were introduced [6, 12, 13] in order to describe the circumferential magnetic anisotropy in amorphous wires. It was established that to achieve high GMI effect, the magnetic anisotropy should be as small as possible.

From the point of view of industrial applications, low hysteretic GMI effect with linear magnetic field dependence of the output signal are desirable [6, 8]. Antisymmetrical magnetic field dependence of the output voltage with linear region has been obtained for pulsed GMI effect based on detection of the off-diagonal GMI component of amorphous wires [6, 8, 12]. Such pulsed scheme for GMI measurements resulted quite useful for real GMI sensors development [8].

Magnetic anisotropy of amorphous microwires in the absence of magnetocrystalline anisotropy is determined mostly by the magnetoelastic term [15–19]. Therefore, the

magnetic anisotropy can be tailored by thermal treatment [15, 20]. On the other hand, recently considerable GMI hysteresis has been observed and analyzed in microwires. This GMI hysteresis has been explained through the helical magnetic anisotropy [21].

Consequently, in this paper, we studied the GMI effect (GMI ratio,  $\Delta Z/Z$ , diagonal  $Z_{zz}$ , and off-diagonal impedance tensor  $Z_{\phi_z}$  components) and hysteretic magnetic properties in ultra-thin amorphous glass-coated microwires with vanishing magnetostriction constant and report results on correlation of the GMI effect with magnetic anisotropy and possibilities to tailor magnetic field dependence of the GMI effect.

## 2 Experimental Details

We studied microwires with nominal compositions  $\text{Co}_{67.1}\text{Fe}_{3.8}\text{Ni}_{1.4}\text{Si}_{14.5}\text{B}_{11.5}\text{Mo}_{1.7}$ ,  $\text{Co}_{66.87}\text{Fe}_{3.66}\text{C}_{0.98}\text{Si}_{11.47}\text{B}_{13.36}\text{Mo}_{1.52}$ , and  $\text{Co}_{66}\text{Cr}_{3.5}\text{Fe}_{3.5}\text{B}_{16}\text{Si}_{11}$  different diameters of metallic nucleus,  $d$ , total diameters,  $D$ , and consequently different  $\rho$ -ratios ( $\rho = d/D$ ) fabricated by the Taylor–Ulitsky method [6, 7, 15].

It is worth mentioning that the strength of internal stresses is determined by ratio  $\rho$  [6, 19, 22]. Therefore, controllable change of the  $\rho$ -ratio allowed us to control residual stresses.

The magnetoelastic energy,  $K_{\text{me}}$ , is given by

$$K_{\text{me}} \approx 3/2\lambda_s\sigma, \quad (1)$$

where  $\sigma = \sigma_i + \sigma_a$ —total stress,  $\sigma_i$ —are the internal stresses,  $\sigma_a$ —applied stresses, and  $\lambda_s$ —magnetostriction constant [6].

In this way, we studied the effect of magnetoelastic contribution on soft magnetic properties and GMI effect of microwires controlling the magnetostriction constant, applied and/or residual stresses.

We have measured dependences of the diagonal  $Z_{zz}$  and off-diagonal  $Z_{\phi_z}$  impedance components and the GMI ratio,  $\Delta Z/Z$ , on external axial magnetic field  $H$  in Co-rich microwires, as described elsewhere [6, 21]. We use a specially designed microstrip cell previously described elsewhere [21, 23]. The components  $Z_{zz}$  and  $Z_{\phi_z}$  were measured simultaneously using a vector network analyzer. The diagonal impedance of the sample  $Z_w = Z_{zz}l$ , where  $l$  is the wire length was obtained from reflection coefficient  $S_{11}$  and the off-diagonal impedance  $Z_{\phi_z}$  was measured as transmission coefficient  $S_{21}$  as a voltage induced in a 2-mm long pick-up coil wound over the wire. The static bias field  $H_B$  was created by the  $d_c$  current  $I_B$  applied to sample through the bias-tee element. The frequency range for the off-diagonal component  $Z_{\phi_z}$  was 10–300 MHz, while the diagonal impedance component has been measured until 7 GHz.

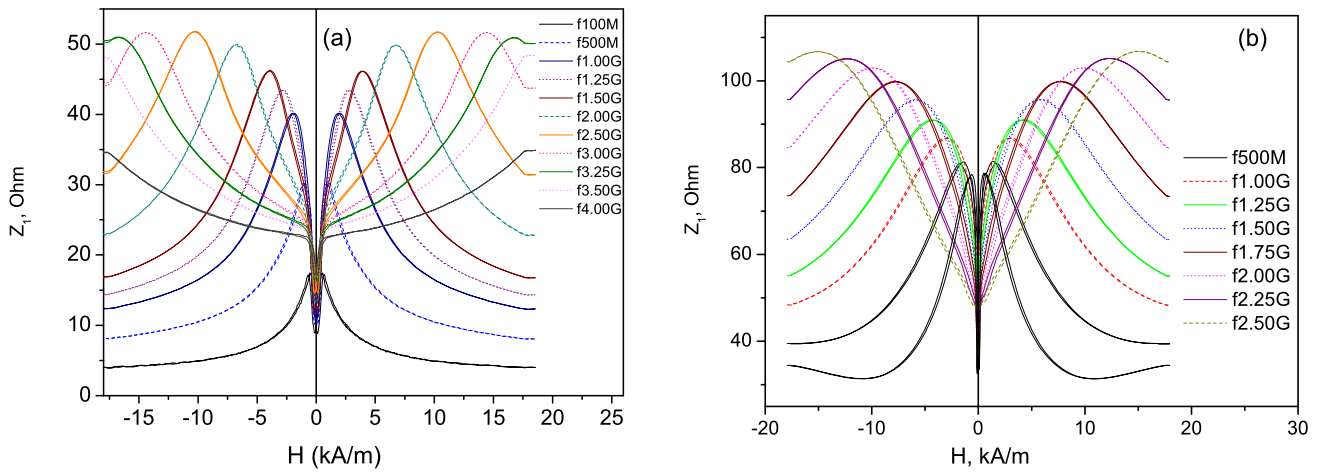


**Fig. 1**  $Z_1(H)$  dependence of  $\text{Co}_{66}\text{Cr}_{3.5}\text{Fe}_{3.5}\text{B}_{16}\text{Si}_{11}$  (a) and  $\text{Co}_{67}\text{Fe}_{3.85}\text{Ni}_{1.45}\text{B}_{11.5}\text{Si}_{14.5}\text{Mo}_{1.7}$  (b) microwires measured at different frequencies

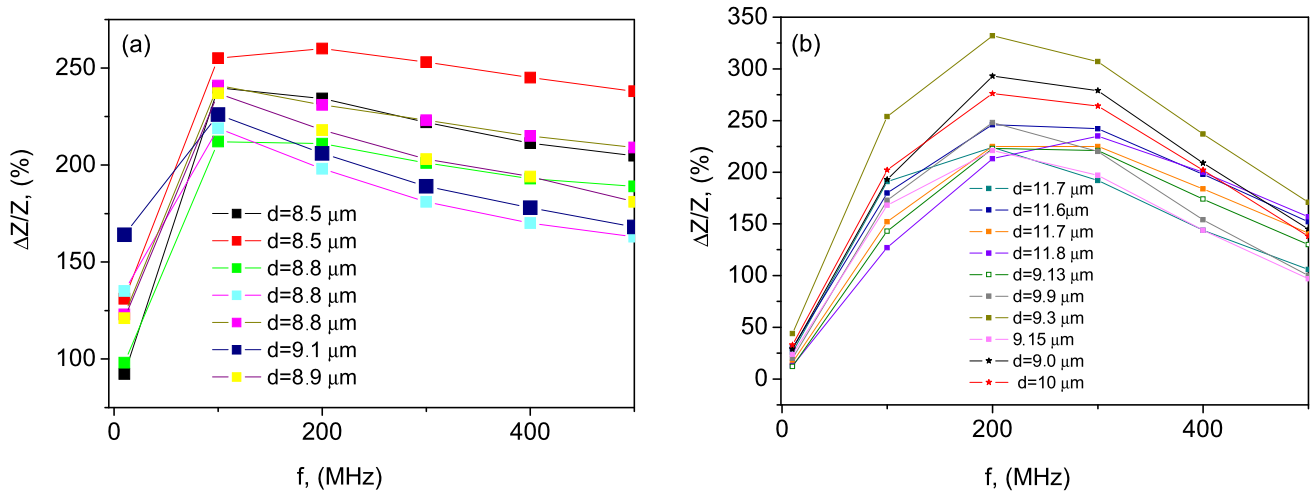


**Fig. 2** Frequency dependence of  $\text{Co}_{66.87}\text{Fe}_{3.66}\text{C}_{0.98}\text{Si}_{11.47}\text{B}_{13.36}\text{Mo}_{1.52}$  microwires with different metallic nucleus diameters

For practical sensor, the pulsed excitation is preferred over sinusoidal because of simple electronic design and low power consumption, therefore, we studied also the pulsed GMI effect using pulsed excitation scheme, as described elsewhere [6, 12, 13].

Hysteresis loops have been measured by the induction method, as described elsewhere [6].

### 3 Experimental Details and Discussion

#### 3.1 Frequency Dependence of GMI Effect

Magnetic field,  $H$ , dependence of real part,  $Z_1$  of the longitudinal wire impedance  $Z_{zz}$  ( $Z_{zz} = Z_1 + iZ_2$ ), measured up to 4 GHz in  $\text{Co}_{66}\text{Cr}_{3.5}\text{Fe}_{3.5}\text{B}_{16}\text{Si}_{11}$  and  $\text{Co}_{67}\text{Fe}_{3.85}\text{Ni}_{1.45}\text{B}_{11.5}\text{Si}_{14.5}\text{Mo}_{1.7}$  microwires are shown in Fig. 1. General features of these dependences are existence of two maxima that shift to higher magnetic fields with increasing

the frequency,  $f$ . Considerable GMI effect has been observed even at GHz-range frequencies. On the other hand, if the maximum applied magnetic field is not high enough, impedance change induced by applied magnetic field at high frequencies decreases starting from some frequency.

For example, most of the studied microwires show the highest GMI ratio at frequencies between 100 and 300 MHz (see Fig. 2). Other interesting features observed in Figs. 2a, b are that the frequency dependence of maximum GMI ratio,  $\Delta Z/Z_m(f)$ , measured in microwires of the same composition and different diameters present an optimum frequency (at which  $\Delta Z/Z_m$  versus  $f$  exhibits the maximum) at different frequencies. Thus, for metallic nucleus diameters ranging between 8.5 and 9.0  $\mu\text{m}$ , the optimal frequency is about 100 MHz, while for microwires with metallic nucleus diameters between 9 and 11.7  $\mu\text{m}$  the optimal frequency is about 200 MHz.

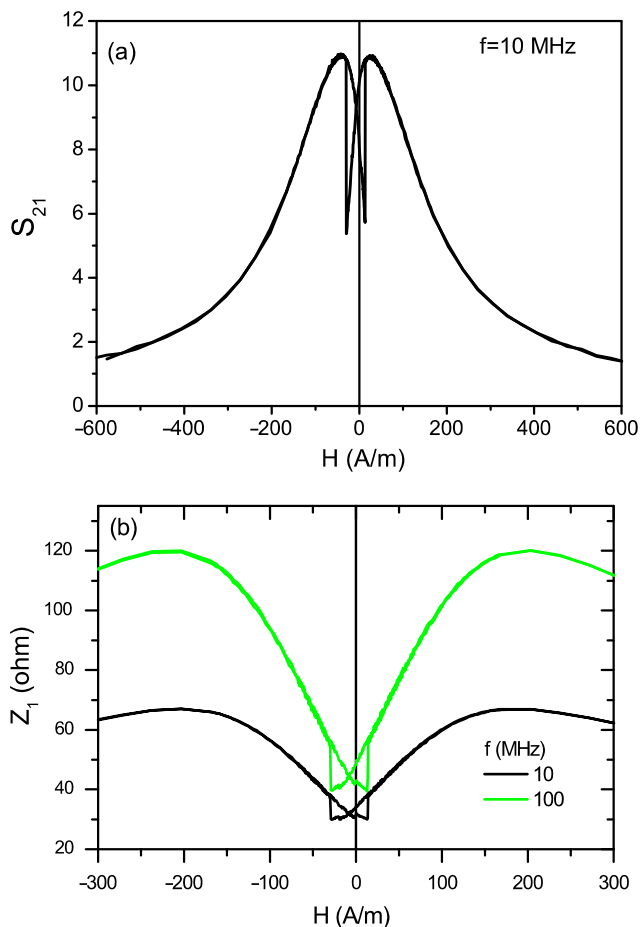


**Fig. 3** Magnetic field dependences of the coefficient  $S_{21}$  at 10 MHz (a) and  $Z_1(H)$  dependences at different frequencies (b) measured in  $\text{Co}_{67}\text{Fe}_{3.85}\text{Ni}_{1.45}\text{B}_{11.5}\text{Si}_{14.5}\text{Mo}_{1.7}$  microwire

Off-diagonal and diagonal components of GMI, measured in  $\text{Co}_{67}\text{Fe}_{3.85}\text{Ni}_{1.45}\text{B}_{11.5}\text{Si}_{14.5}\text{Mo}_{1.7}$  microwires are shown in Fig. 3. As can be appreciated from Fig. 3, considerable hysteresis for both off-diagonal and longitudinal impedance is observed for studied microwires. It is important that the GMI hysteresis does not depend on frequency: increasing the frequency the GMI hysteresis persists (Fig. 3b). It is worth mentioning that usually the DC magnetic field that corresponds to the maximum GMI ratio,  $H_m$ , is attributed to the static magnetic anisotropy field,  $H_k$ .

As regarding to the origin of the frequency dependence of  $H_m$ , observed in Fig. 1 for both microwires, there are different points of view. Experimentally, we observed that the magnetic field at which the maximum occurs considerable increase with frequency,  $f$ .

The possible explanation for this is that the magnetic structure and the anisotropy can be different near the surface. At higher frequencies, the current flows closer to the surface, then the effective anisotropy field and dispersion can change with frequency. Another reason might be con-

nected with the frequency dependence of the domain wall permeability.

Another interpretation is related with close analogy between giant magnetoimpedance and ferromagnetic resonance, as previously reported elsewhere [5, 23]. Indeed, saturation magnetization can be estimated from the equation

$$M_s = 0.805 \times 10^{-9} df_0^2/dH \quad (2)$$

where  $f$  is the resonant frequency,  $H$  is the applied magnetic field, and  $M_s$  is the saturation magnetization. This approach predicts the linear relation between the square of the resonance frequency and the applied field,  $f_0^2(H)$ . Our experimental data for two  $\text{Co}_{67.05}\text{Fe}_{3.85}\text{Ni}_{1.4}\text{B}_{11.33}\text{Si}_{14.47}\text{Mo}_{1.69}$  microwire samples with different  $\rho$ -ratios fits well with the predicted linear dependence (see Figs. 4b, d).

The saturation magnetization values, obtained from (2) give us quite reasonable values of about 0.5–0.53 MA/m.

Consequently, we observed considerable GMI effect at GHz-range frequencies in studied microwires (Figs. 1, 4a, c). Therefore, developed materials are useful for engineering of tunable metamaterials where the GMI effect in microwires embedded into dielectric matrix is used to control the effective electromagnetic properties of composite material [6, 24]. On the other hand, frequency dependence of GMI effect at GHz frequencies fits well with ferromagnetic resonance behavior, as previously reported elsewhere [23, 25].

### 3.2 Effect of Magnetoelastic Anisotropy and GMI Hysteresis

As mentioned above, the internal stresses,  $\sigma_1$ , arising during simultaneous rapid quenching of metallic nucleus surrounding by the glass coating are the source of additionally magnetoelastic anisotropy. The strength of such internal stresses can be controlled by the  $\rho$ -ratio: strength of internal stresses increases decreasing  $\rho$ -ratio (i.e., increases with increasing of the glass volume) [17–19].

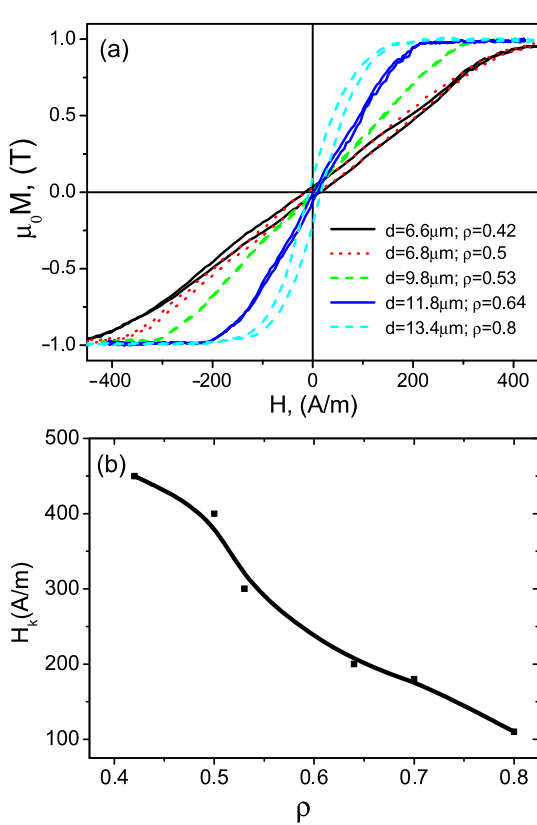
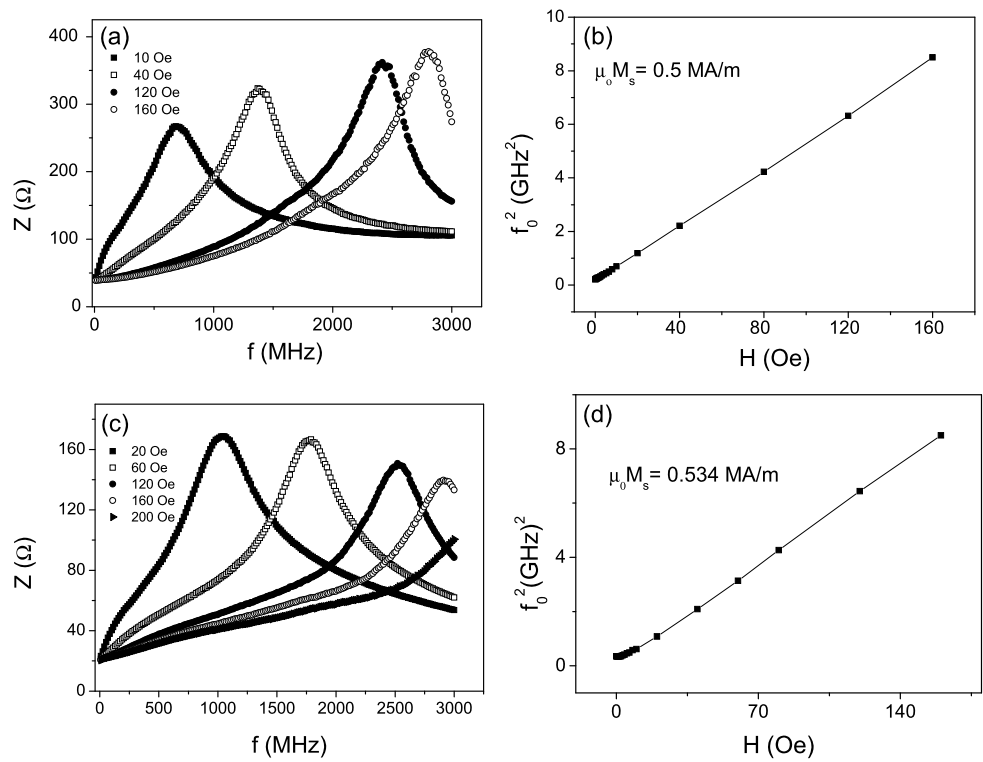
Consequently, the parameter  $\rho$  must be considered as one of the factors that affect both soft magnetic properties and GMI.

Figure 5 shows the influence of the  $\rho$ -ratio on hysteresis loops and magnetic anisotropy field of  $\text{Co}_{67.1}\text{Fe}_{3.8}\text{Ni}_{1.4}\text{Si}_{14.5}\text{B}_{11.5}$  microwires with the same composition of the metallic nucleus, but different  $\rho$ -ratio.

As can be appreciated, all studied samples exhibited excellent magnetically soft properties with low coercivities (between 4 and 10 A/m). Magnetic anisotropy field,  $H_k$ , is found to be determined by the  $\rho$ -ratio, decreasing with  $\rho$  (Fig. 5b), as previously reported [6].

Consequently, one can expect that the  $\rho$ -ratio must affect the GMI effect of studied samples.

**Fig. 4** Frequency dependence of GMI effect (a, c) and  $f_0^2(H)$  dependence (b, d) measured for  $\text{Co}_{67.05}\text{Fe}_{3.85}\text{Ni}_{1.4}\text{B}_{11.33}\text{Si}_{14.47}\text{Mo}_{1.69}$  microwires with  $d \approx 16.2 \mu\text{m}$ ,  $\rho \approx 0.7$ , and  $d = 21.4$ ,  $\rho \approx 0.816$ , respectively



**Fig. 5** Hysteresis loops of  $\text{Co}_{67.1}\text{Fe}_{3.8}\text{Ni}_{1.4}\text{Si}_{14.5}\text{B}_{11.5}\text{Mo}_{1.7}$  microwires with different geometry (a) and dependence of  $H_k$  on  $\rho$ -ratio (b)

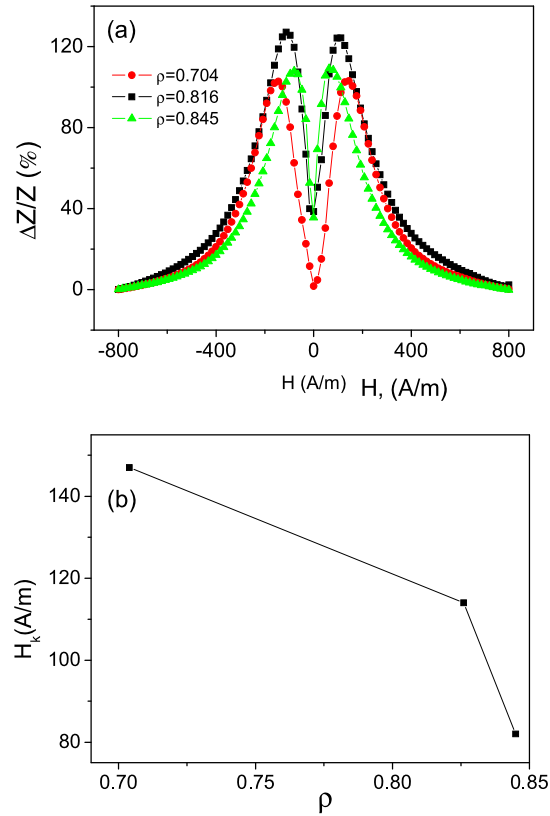


**Fig. 6** Effect of  $\rho$ -ratio on GMI effect in  $\text{Co}_{67.05}\text{Fe}_{3.85}\text{Ni}_{1.4}\text{B}_{11.33}\text{Si}_{14.47}\text{Mo}_{1.69}$  microwire samples with different  $\rho$ -ratios (a) and dependence of field of maximums on  $\rho$ -ratio (b)

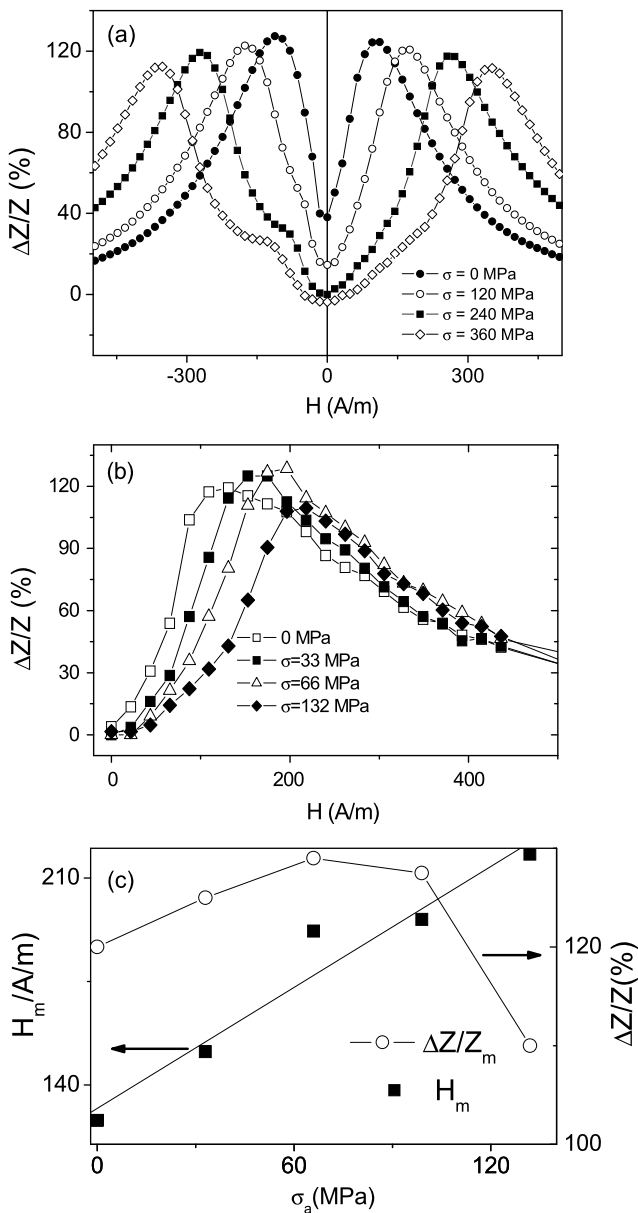


**Fig. 7**  $\Delta Z/Z(H)$  dependences of  $\text{Co}_{67.05}\text{Fe}_{3.85}\text{Ni}_{1.4}\text{B}_{11.33}\text{Si}_{14.47}\text{Mo}_{1.69}$  (a) and  $\text{Co}_{68.5}\text{Mn}_{6.5}\text{Si}_{10}\text{B}_{15}$  (b) amorphous microwires measured at different  $\sigma_a$  and  $H_m(\sigma)$  dependence for  $\text{Co}_{68.5}\text{Mn}_{6.5}\text{Si}_{10}\text{B}_{15}$  amorphous microwire (c)

Figure 6 presents results on magnetic field dependences of  $\Delta Z/Z$  measured in  $\text{Co}_{67.05}\text{Fe}_{3.85}\text{Ni}_{1.4}\text{B}_{11.33}\text{Si}_{14.47}\text{Mo}_{1.69}$  microwire samples with different  $\rho$ -ratios.

Indeed, both maximum values of the GMI ratio,  $\Delta Z/Z_m$ , and the magnetic anisotropy field present considerable dependence on samples geometry. It is worth mentioning that for similar microwires composition  $\Delta Z/Z_m \approx 600\%$  has been observed for optimized microwire geometry factors ( $\rho$ -ratio) [6, 26].

Considering that the magnetoelastic energy,  $K_{me}$ , is determined by both internal,  $\sigma_i$ , and applied stresses,  $\sigma_a$ , we

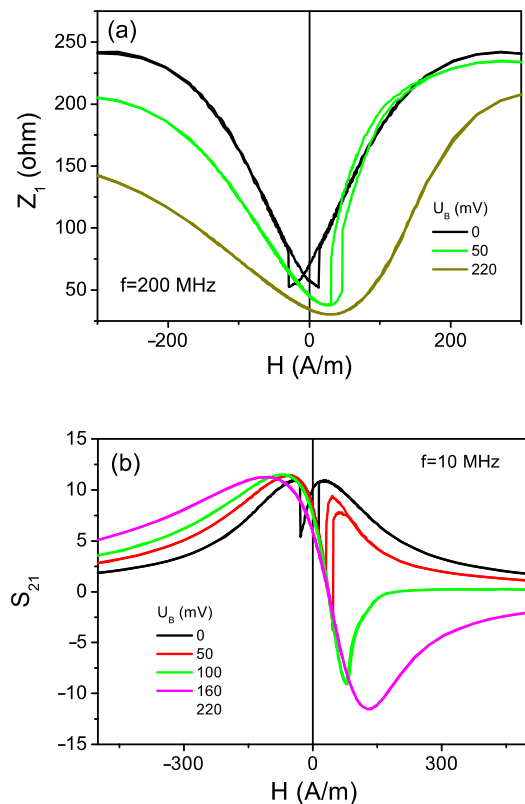


**Fig. 8** Effect of bias voltage  $U_B$  on magnetic field dependence of diagonal impedance measured at 200 MHz (a) and  $S_{21}$  parameter measured at 10 MHz (b) of  $\text{Co}_{67}\text{Fe}_{3.85}\text{Ni}_{1.45}\text{B}_{11.5}\text{Si}_{14.5}\text{Mo}_{1.7}$  microwire

measured the GMI effect under tensile stresses in various Co-rich microwires. Figure 7 presents tensile stress dependence measured in  $\text{Co}_{67.05}\text{Fe}_{3.85}\text{Ni}_{1.4}\text{B}_{11.33}\text{Si}_{14.47}\text{Mo}_{1.69}$  and  $\text{Co}_{68.5}\text{Mn}_{6.5}\text{Si}_{10}\text{B}_{15}$  microwires. We observed that  $\Delta Z/Z$  and  $H_m$  are quite sensitive to the application of external tensile stresses,  $\sigma_a$ : Here, the magnetic field,  $H_m$  corresponding to the maximum of  $(\Delta Z/Z)$  shows a roughly linear increase with  $\sigma$  (Fig. 7c). From the  $H_m(\sigma)$  dependence exhibiting a slope of around  $0.7 \text{ A}/(\text{m} \times \text{MPa})$ , we estimated the unstressed value of the saturation magnetostriction constant,  $\lambda_{s,0}$ . Estimated  $\lambda_{s,0} \approx -2 \times 10^{-7}$  values are rather reasonable in comparison with the reported values measured from the stress dependence of initial magnetic susceptibility ( $\lambda_{s,0} \approx -3 \times 10^{-7}$  for such composition) and the magnetostriction values measured in amorphous wires of similar compositions [6, 11, 27].

In fact, the tendency on the change of  $H_m$  under application of tensile stresses (Fig. 8c) and the change of  $H_m$  and  $H_k$  with decreasing the  $\rho$ -ratio (Figs. 6, 7) is the same that confirms the effect of magnetoelastic anisotropy on hysteresis loops and GMI effect.

It is worth mentioning that in some cases the value of maximum GMI ratio  $(\Delta Z/Z)_m$  has a nonmonotonic dependence on  $\sigma$  (either applied or internal) exhibiting a broad maximum at around 60 MPa ( $(\Delta Z/Z)_m \approx 130\%$ )

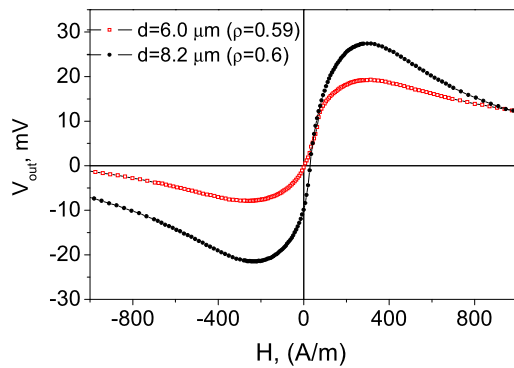


**Fig. 9**  $V_{out}(H)$  response of  $\text{Co}_{67.1}\text{Fe}_{3.8}\text{Ni}_{1.4}\text{Si}_{14.5}\text{B}_{11.5}\text{Mo}_{1.7}$  microwires with different diameters,  $d$ , and  $\rho$ -ratios

for  $\text{Co}_{68.5}\text{Mn}_{6.5}\text{Si}_{10}\text{B}_{15}$  microwire (Fig. 7c) or exhibiting a maximum at intermediate  $\rho$ -ratio values (Fig. 6a).

Our recent studies reveal that the easy magnetization axis of Co-rich microwires is often considerable deviated from the transversal direction. Thus, we explained the nature of observed low field hysteresis on  $Z_1(H)$  and  $Z_{\varphi z}(H)$  (Figs. 3a and 3b) considering the existence of helical magnetic anisotropy [21]. Consequently, application of circular bias magnetic field  $H_B$  produced by DC current  $I_B$  running through the wire affects the hysteresis and asymmetry of the MI dependence, suppressing this hysteresis when  $I_B$  is high enough (see Fig. 8, where effect of bias voltage on diagonal impedance,  $Z_1$ , and on  $S_{21}$  parameter, proportional to off-diagonal GMI component is shown).

### 3.3 Pulsed GMI Effect

As mentioned above, antisymmetrical magnetic field dependence of the output voltage with monotonic magnetic field dependence at zero-field region can be obtained for pulsed excitation regime. The output voltage from the pick-up coil surrounding microwire is proportional to the off-diagonal GMI component of amorphous wires. Figure 9 shows field dependence of the off-diagonal voltage response,  $V_{out}$  measured using pulsed scheme, in  $\text{Co}_{67.1}\text{Fe}_{3.8}\text{Ni}_{1.4}\text{Si}_{14.5}\text{B}_{11.5}\text{Mo}_{1.7}$  ( $\lambda_s \approx -3 \times 10^{-7}$ ) microwire with different geometry: metallic nucleus diameter of 6  $\mu\text{m}$  and total diameter 10.2  $\mu\text{m}$  ( $\rho \approx 0.59$ ) and metallic nucleus diameter of 8.2  $\mu\text{m}$  total diameter of 13.7  $\mu\text{m}$  ( $\rho \approx 0.6$ ). Observed antisymmetrical magnetic field dependence can be suitable for determination the magnetic field direction in real sensor devices [6, 12]. It should be noted from Fig. 9 that the  $V_{out}(H)$  curves exhibit nearly linear growth within the field range from  $-H_m$  to  $H_m$ . The  $H_m$  (about 240 A/m) limits the working range of MI sensor. As can be observed, the amplitude of the  $V_{out}$  increases with increasing the metallic nucleus diameter,  $d$ . On the other hand, the  $H_m$  value depends on the microwires geometry.

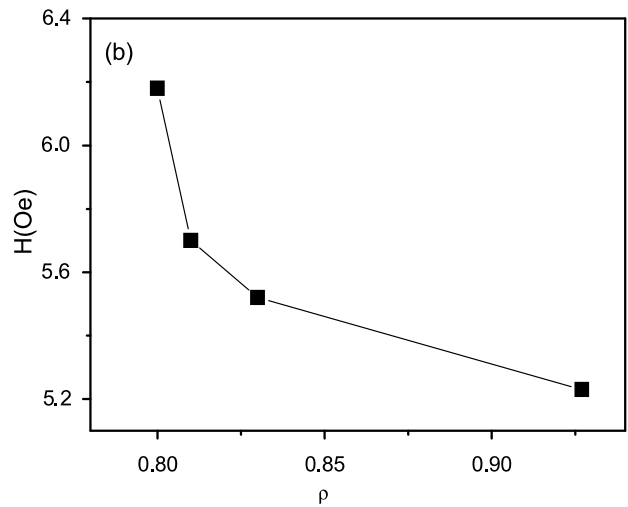
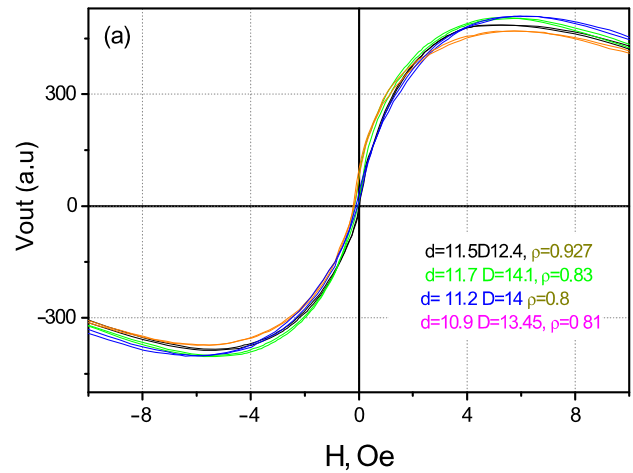


**Fig. 10**  $V_{out}(H)$  response of  $\text{Co}_{67.71}\text{Fe}_{4.28}\text{Ni}_{1.57}\text{B}_{12.4}\text{Si}_{11.24}\text{Mo}_{1.25}$  with similar metallic nucleus diameters,  $d$ , and different  $\rho$ -ratios (a) and  $H(\rho)$  dependence (b)

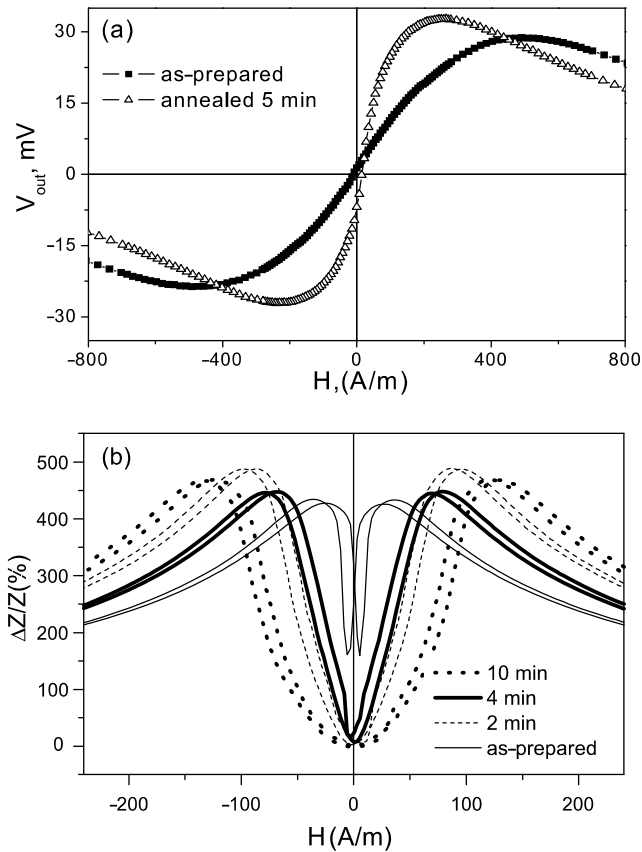
Figure 10 shows  $V_{out}(H)$  dependences measured for  $\text{Co}_{67.71}\text{Fe}_{4.28}\text{Ni}_{1.57}\text{B}_{12.4}\text{Si}_{11.24}\text{Mo}_{1.25}$  microwires with similar  $d$ -values but with different  $\rho$ -ratios. As observed in Fig. 10b,  $H_m$  decrease increasing  $\rho$ -ratios.  $H_m$  should be associated with the magnetic anisotropy field. Like in the case of conventional GMI effect, the effect of the  $\rho$ -ratio on  $V_{out}(H)$  (Fig. 10b) should be attributed to the magnetoelastic anisotropy related with the internal stresses.

Since the magnetostriction constant given by (1) is mostly determined by the chemical composition and achieves almost nearly-zero values in amorphous alloys based on Fe–Co with  $\text{Co/Fe} \approx 70/5\lambda_s \approx 0$  [6, 11], the effect of the internal stresses determined by the  $\rho$ -ratio must be taken into account.

Additionally, to the composition and geometrical factors, the magnetoelastic anisotropy can be also be tailored by reducing the internal stresses through the application of heat treatment.

### 3.4 Manipulation of GMI Effect and Magnetic Properties by Heat Treatments

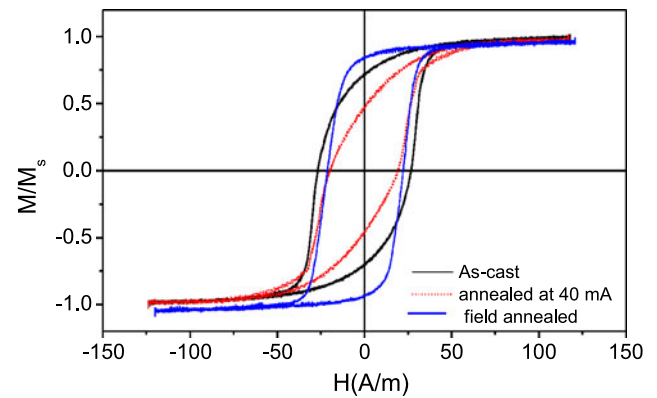
The influence of Joule heating on off-diagonal field characteristic of nearly zero magnetostriction  $\text{Co}_{67}\text{Fe}_{3.85}\text{Ni}_{1.45}\text{B}_{11.5}\text{Si}_{14.5}\text{Mo}_{1.7}$  microwire with diameters 9.4/17.0  $\mu\text{m}$  ( $\rho \approx 0.55$ ) is shown in Fig. 11a. One can see that the thermal annealing with 50 mA DC current reduces the  $H_m$  from 480 A/m in as-cast state to 240 A/m after 5 min annealing.



**Fig. 11**  $V_{out}(H)$  of as-prepared and Joule-heated  $\text{Co}_{67}\text{Fe}_{3.85}\text{Ni}_{1.45}\text{B}_{11.5}\text{Si}_{14.5}\text{Mo}_{1.7}$  microwire (current annealing with 50 mA current intensity) (a) and  $\Delta Z/Z(H)$  dependences of heated  $\text{Co}_{67}\text{Fe}_{3.85}\text{Ni}_{1.45}\text{B}_{11.5}\text{Si}_{14.5}\text{Mo}_{1.7}$  microwire measured at  $f = 30$  MHz and  $I = 1$  mA in microwire subjected to CA annealing at 40 mA for different time (b)

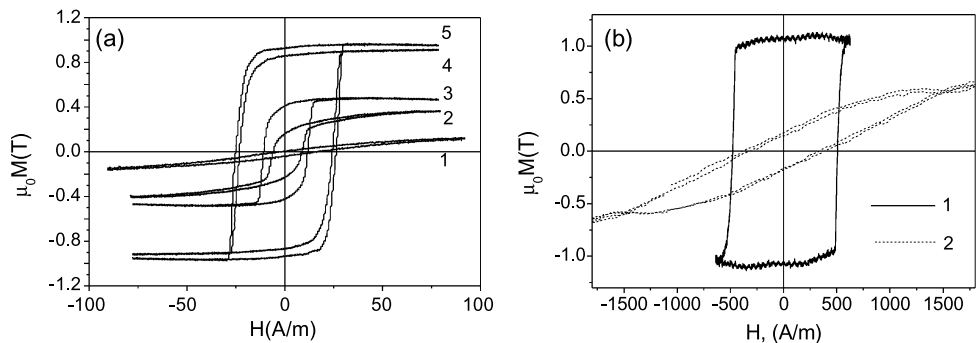
Similarly, current annealing (due to Joule heating) induced changes in GMI response (Fig. 11b). This effect should be mostly attributed to the stress relaxation (although electrical current also induce circular magnetic field).

As demonstrated before, application of stress and/or magnetic field during annealing of amorphous materials may induce strong additional magnetic anisotropy. In the case of microwires, this induced anisotropy can be reinforced due to strong internal stresses (therefore even conventional annealing must be considered as stress-annealing) [20, 22]. In some cases, this results in drastic changes of hysteretic magnetic properties and GMI behavior [15, 21]. As an example, application of axial magnetic field during annealing induces axial magnetic anisotropy in Co-rich microwires (Fig. 12). Here hysteresis loops of  $\text{Co}_{67}\text{Fe}_{3.85}\text{Ni}_{1.45}\text{B}_{11.5}\text{Si}_{14.5}\text{Mo}_{1.7}$  microwires ( $d = 22.4 \mu\text{m}$ ,  $D = 22.8 \mu\text{m}$ ) annealed by Joule heating without (CA) and under application of axial magnetic field (FCA) are shown. As can be appreciated, application of magnetic field during annealing completely resulted in the opposite tendency in changing of magnetic properties induced by annealing: increasing of remanent magnetization and decreasing of coercivity after FCA is observed, while CA treatment induced decreasing of the remanence and of the coercivity.



**Fig. 12** Effect of CA and FCA on hysteresis loops of  $\text{Co}_{67}\text{Fe}_{3.85}\text{Ni}_{1.45}\text{B}_{11.5}\text{Si}_{14.5}\text{Mo}_{1.7}$  microwires ( $d = 22.4 \mu\text{m}$ ,  $D = 22.8 \mu\text{m}$ )

**Fig. 13** Hysteresis loops of  $\text{Fe}_{74}\text{B}_{13}\text{Si}_{11}\text{C}_2$  microwire annealed under applied stress of 500 MPa (a) at (1)—300 °C 3 hours, (2)—280 °C 40 min, (3)—265 °C 40 min, (4)—235 °C 40 min, and (5)—215 °C 40 min and (b) stress induced changes of hysteresis loops of the same microwires (1—measured under applied stress, 2—measured without stress)





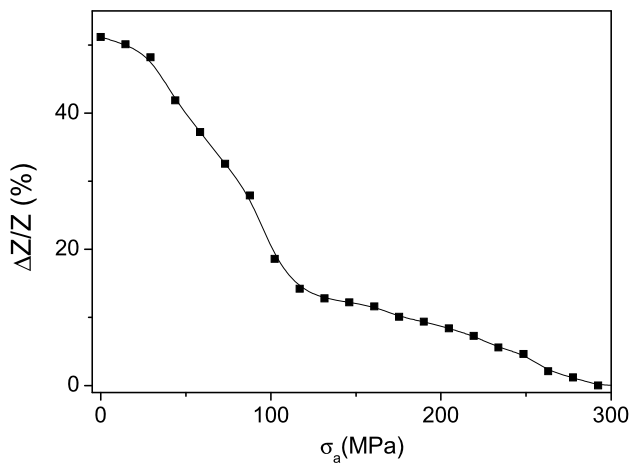


**Fig. 14** Stress impedance effect of stress annealed  $\text{Fe}_{74}\text{B}_{13}\text{Si}_{11}\text{C}_2$  glass-coated microwire under stress (468 MPa) at 275 °C for 0.5 h measured at frequency,  $f = 10$  MHz for the driving current amplitude of 2 mA

In the case of Fe-rich microwires subjected to the annealing in the presence of tensile stresses complete change of magnetic anisotropy can be realized (Fig. 13). Stress annealing of  $\text{Fe}_{74}\text{B}_{13}\text{Si}_{11}\text{C}_2$  microwires resulted in induction of considerable stress induced anisotropy [20]. The shape of hysteresis loop completely changes and the strength of induced changes depends on time and temperature of annealing (Fig. 13a). In this case, the easy axis of magnetic anisotropy has been changed from axial to transversal [20]. Additionally, application of stress during measurements of stress-annealed microwires with well-defined transverse anisotropy results in drastic change of the hysteresis loop (Fig. 13b).

Origin of such stress-induced anisotropy is related with so-called “back stresses” originated from the composite origin of glass-coated microwires annealed under tensile stress: compressive stresses compensate axial stress component and under these conditions transversal stress components are predominant [20].

Consequently, these stress annealed samples exhibit stress-impedance effect, i.e., impedance change ( $\Delta Z/Z$ ) under applied stress,  $\sigma$ , observed in samples with stress induced transversal anisotropy (see Fig. 14) [20].

It should be assumed that the internal stresses relaxation after heat treatment should drastically change both the soft magnetic behavior and the  $\Delta Z/Z(H)$  dependence due to the stress relaxation, induced magnetic anisotropy and change of the magnetostriction constant under annealing.

#### 4 Conclusions

In thin amorphous wires, produced by the Taylor–Ulitsky technique, magnetic softness and magnetic field dependence

of GMI effect (both longitudinal and off-diagonal) and GMI hysteresis are determined the magnetoelastic anisotropy. This magnetoelastic anisotropy can be manipulated by the sample geometry and adequate annealing. There are a number of interesting effects, such as induction of the transversal anisotropy in Fe-rich microwires allowing observation of the stress-impedance effect and stress sensibility of overall hysteresis loop shape. Observed low-field GMI hysteresis can be suppressed by the bias electrical current.

Studies of diagonal and off-diagonal MI tensor components of glass-coated microwires have shown the great potential of these materials for microminiaturized magnetic field sensor application. Their main advantages are high sensitive low-hysteresis field dependence. By varying the alloys composition and applying post fabrication processing, it is possible to control the sensor’s operating range. Low field GMI hysteresis has been observed and explained in terms of helical magnetic anisotropy of microwires.

**Acknowledgements** This work was supported by EU ERA-NET programme under project “SoMaMicSens” (MANUNET-2010-Basque-3), by EU under FP7 “EM-safety” project, by the Spanish Ministry of Science and Innovation, MICINN under Project MAT2010-18914, by the Basque Government under Saiotek 2011 MIMAGURA project (S-PE11UN087), Saiotek-2011 MAGNANEL (S-E11UN085) and Saiotek-2012 MEMFOMAG (S-PE12UN139), and by federal target program “Scientific and scientific-pedagogical personnel of innovative Russia,” state contract no. 14.A18.21.0783.

#### References

1. Phan, M.-H., Peng, H.-X.: Prog. Mater. Sci. **53**, 323 (2008)
2. Mohri, K., Humphrey, F.B., Kawashima, K., Kimura, K., Muzutani, M.: IEEE Trans. Magn. **26**, 1789 (1990)
3. Zhukov, A.P.: Mater. Des. **14**, 299 (1993)
4. Zhukova, V., Zhukov, A., Kraposhin, V., Prokoshin, A., Gonzalez, J.: Sens. Actuators A **106**, 225 (2003)
5. Ciureanu, P., Rudkowska, G., Clime, L., Sklyuyev, A., Yelon, A.: J. Optoelectron. Adv. Mater. **6**, 905 (2004)
6. Zhukova, V., Ipatov, M., Zhukov, A.: Sensors **9**, 9216 (2009)
7. Vazquez, M., Chiriac, H., Zhukov, A., Panina, L., Uchiyama, T.: Phys. Status Solidi A **208**, 493 (2011)
8. Honkura, Y.: J. Magn. Magn. Mater. **249**, 375 (2002)
9. Panina, L.V., Mohri, K.: Appl. Phys. Lett. **65**, 1189 (1994)
10. Beach, R., Berkowitz, A.: Appl. Phys. Lett. **64**, 3652 (1994)
11. Konno, Y., Mohri, K.: IEEE Trans. Magn. **25**(5), 3623 (1989)
12. Sandacci, S.I., Makhnovskiy, D.P., Panina, L.V., Mohri, K., Honkura, Y.: IEEE Trans. Magn. **35**, 3505 (2004)
13. Usov, N.A., Antonov, A.S., Lagar’kov, A.N.: J. Magn. Magn. Mater. **185**, 159 (1998)
14. Makhnovskiy, D.P., Panina, L.V., Mapps, D.J.: Phys. Rev. B **63**, 1444241 (2001)
15. Zhukov, A., Zhukova, V.: Magnetic properties and applications of ferromagnetic microwires with amorphous and nanocrystalline structure. Nova Science Publishers, Inc., Hauppauge (2009). 162 p. ISBN 978-1-60741-770-5
16. Zhukova, V., Usov, N.A., Zhukov, A., Gonzalez, J.: Phys. Rev. B **65**, 134407 (2002)
17. Chiriac, H., Ovari, T.A., Pop, Gh.: Phys. Rev. B **42**, 10105 (1995)

18. Antonov, A.S., Borisov, V.T., Borisov, O.V., Prokoshin, A.F., Usov, N.A.: *J. Phys. D, Appl. Phys.* **33**, 1161 (2000)
19. Chiriac, H., Ovari, T.-A., Zhukov, A.: *J. Magn. Magn. Mater.* **254–255**, 469 (2003)
20. Zhukov, A.: *Adv. Funct. Mater.* **16**, 675 (2006)
21. Ipatov, M., Zhukova, V., Zhukov, A., Gonzalez, J., Zvezdin, A.: *Phys. Rev. B* **81**, 134421 (2010)
22. Zhukov, A.: *J. Magn. Magn. Mater.* **242–245**, 216 (2002)
23. Ménard, D., Britel, M., Ciureanu, P., Yelon, A.: *J. Appl. Phys.* **84**, 2805 (1998)
24. Ipatov, M., Aranda, G.R., Zhukova, V., Panina, L.V., González, J., Zhukov, A.: *Appl. Phys. A, Mater. Sci. Process.* **103**, 693 (2011)
25. García, C., Zhukov, A., Zhukova, V., Ipatov, M., Blanco, J.M., Gonzalez, J.: *IEEE Trans. Magn.* **41**, 3688 (2005)
26. Zhukova, V., Chizhik, A., Zhukov, A., Torcunov, A., Larin, V., Gonzalez, J.: *IEEE Trans. Magn.* **38**, 3090 (2002)
27. Cobeño, A.F., Zhukov, A., Blanco, J.M., Gonzalez, J.: *J. Magn. Magn. Mater.* **234**, L359 (2001)